

Supporting Information for

**Chiral supramolecular coordination cages as high-performance
inhibitors against amyloid- β aggregation**

*Ling-Yu Bao,^a Si-Jia Hao,^a Sai-Fei Xi,^a Xiaodong Yan,^a Hai-Xia Zhang,^a
Rui Shen,^a Zhi-Guo Gu^{ab*}*

*^a Key Laboratory of Synthetic and Biological Colloids, Ministry of Education, School
of Chemical and Material Engineering, Jiangnan University, Wuxi 214122, China. E-
mail: zhiguogu@jiangnan.edu.cn; Fax: +86 510 85917763; Tel: +86 510 85917090;*

*^b International Joint Research Center for Photoresponsive Molecules and Materials,
School of Chemical and Material Engineering, Jiangnan University, Wuxi 214122,
China*

E-mail: zhiguogu@jiangnan.edu.cn

Table of contents

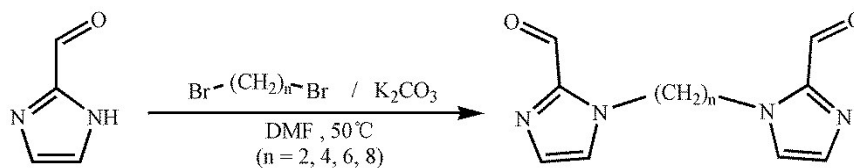
1. Experimental Section	S2
2. Synthesis of a series of dialdehydes	S3
3. NMR spectroscopy of a series of dialdehydes	S5
4. Preparation of cages	S9
5. Mass spectra of cages	S11
6. Stability in aqueous media	S12
7. CD study of Aβ peptide interacting with cages	S13
8. AFM images	S14
9. Thioflavin T fluorescence assay	S16
10. Effect of the cages on ThT fluorescence	S17
11. X-ray crystallography data	S18

1. Experimental Section

The main protein sequence of Alzheimer's disease (AD) H-Asp-Ala-Glu-Phe-Arg-His-Asp-Ser-Gly-TYR-Glu-Val-His-His-Gln-Lys-Leu-Val-Phe-Phe-Ala-Glu-Asp-Val-Gly-Ser-Asn-Lys-Gly-Ala-Ile-Ile-Gly-Leu-Met-Val-Gly-Gly-Val-Val-OH ($A\beta$ 1-40) were synthesized by GL Biochem Ltd, and ThT were purchased from Sigma-Aldrich. Some metal chlorides and tetrafluoroborates were obtained from STREM Chemicals and Energy Chemical. Ultrapure water (18.2 M Ω .cm) was used in all experiments was obtained from a Millipore Milli-Q water system (Bedford, MA, USA). All other reagents employed were of analytical reagent grade or with highest quality, and purchased from commercial sources and used without further purification.

$A\beta$ 1-40 were dissolved in buffers (10 mM NaOH-HCl, pH = 7.4). And the concentrations of $A\beta$ 1-40 were determined by measuring the absorbance at 562 nm in Synergy H4 Hybrid Microplate Reader. Chiral supramolecular coordination cages *1R/1S*, *2R/2S*, *3R/3S* and *4R/4S* were dissolved in DMSO, and a stock solution of 1 mM was prepared. Further dilution was made in the corresponding buffer according to the required concentrations for all the experiments. Infrared spectra were measured with a Nicolet 6700 FT-IR spectrophotometer with ATR attachment in the range of 500-4000 cm⁻¹ region. Element analyses were conducted on elemental corporation vario EL III analyzer. Nuclear magnetic resonance (NMR) spectra were recorded on AVANCE III (400 MHz) instrument at 298 K using standard Bruker software, and chemical shifts were reported in parts per million (ppm) downfield from tetramethylsilane. High-resolution mass spectra (HRMS) were obtained on a Quadrupole-time-of-flight (Q-TOF) mass spectrometer and the fragment voltage was set at 175 V.

2. Synthesis of a series of dialdehydes



Synthesis of 1,2-di(imidazole-2-carboxaldehyde)ethane

Imidazole-2-carboxaldehyde (1.35 g, 14 mmol), 1,2-dibromoethane (0.94 g, 5mmol), and potassium carbonate (1.38 g, 10 mmol) were added to a 50 mL flask containing 20 mL DMF in nitrogen atmosphere. The reaction mixture was stirred at 50 °C for 3 days and then filtered. The filtrate was extracted with ethyl acetate (4×15 mL), collecting the organic phase, washed with saturated aqueous solution of potassium chloride, dried with anhydrous magnesium sulfate, removed the solvent on a rotary evaporator and dried under vacuum in 40 °C to give the desired product as yellow crystals (Yield: 43.41%). Pure light yellow crystals of 1,2-di(imidazole-2-carboxaldehyde)ethane were obtained by recrystallizing the crude product from ethyl acetate. IR (ν cm⁻¹): 3109, 2937, 2848, 1685, 1477, 1413, 1338, 1296, 1245, 1184, 1157, 1083, 921, 802, 756; ESI-MS (m/z): 218.17; Anal. Calcd (%) for C₁₀H₁₀N₄O₂: C, 55.04; H, 4.62; N, 25.68; Found: C, 55.12; H, 4.58; N, 25.71.

Synthesis of 1,4-di(imidazole-2-carboxaldehyde)butane

Compounds of 1,4-di(imidazole-2-carboxaldehyde)butane were prepared by similar procedure to that of 1,2-di(imidazole-2-carboxaldehyde)ethane where 1,4-Dibromobutane (1.08 g, 5 mmol) substituted for 1,2-dibromoethane. The appearance of the product is white needle crystals (Yield: 58.74%). IR (ν cm⁻¹): 3120, 2945, 2858, 2640, 1676, 1475, 1411, 1371, 1334, 1284, 1228, 1180, 1153, 1080, 935, 831, 771; ESI-MS (m/z): 246.03; Anal. Calcd (%) for C₁₂H₁₄N₄O₂: C, 58.53; H, 5.73; N, 22.75; Found: C, 58.49; H, 5.78; N, 22.70.

Synthesis of 1,6-di(imidazole-2-carboxaldehyde)hexane

1,6-di(imidazole-2-carboxaldehyde)hexane were synthesized using the procedure

described for 1,4-di(imidazole-2-carboxaldehyde)butane, substituting 1,6-Dibromohexane (1.22 g, 5 mmol) for 1,4-Dibromobutane. The product is square lamellar crystals (Yield: 46.77%). IR (ν cm^{-1}): 3128, 2941, 2831, 1681, 1471, 1407, 1326, 1263, 1224, 1153, 176, 1004, 918, 826, 771, 690; ESI-MS (m/z): 274.27; Anal. Calcd (%) for $\text{C}_{14}\text{H}_{18}\text{N}_4\text{O}_2$: C, 61.30; H, 6.61; N, 20.42; Found: C, 61.33; H, 6.59; N, 20.45.

Synthesis of 1,8-di(imidazole-2-carboxaldehyde)octane

1,8-di(imidazole-2-carboxaldehyde)octane were synthesized using the procedure described for 1,6-di(imidazole-2-carboxaldehyde)hexane, substituting 1,8-Dibromooctane (1.36 g, 5 mmol) for 1,6-Dibromohexane. The product is cuboid crystals (Yield: 52.18%). IR (ν cm^{-1}): 3128, 2939, 2829, 1681, 1471, 1407, 1328, 1263, 1222, 1155, 1076, 1006, 918, 860, 771, 690; ESI-MS (m/z): 302.01; Anal. Calcd (%) for $\text{C}_{16}\text{H}_{22}\text{N}_4\text{O}_2$: C, 63.55; H, 7.33; N, 18.53; Found: C, 63.58; H, 7.31; N, 18.52.

3. NMR spectroscopy of a series of dialdehydes

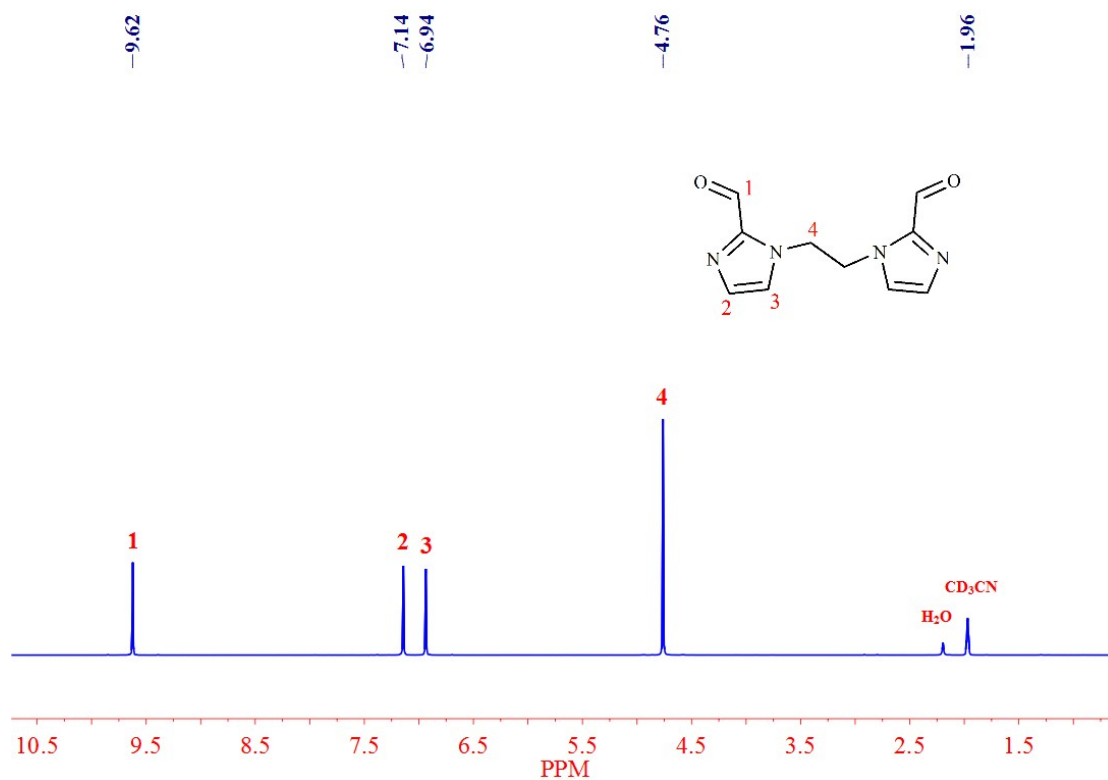


Figure S1. ¹H NMR spectrum of 1,2-di(imidazole-2-carboxaldehyde)ethane

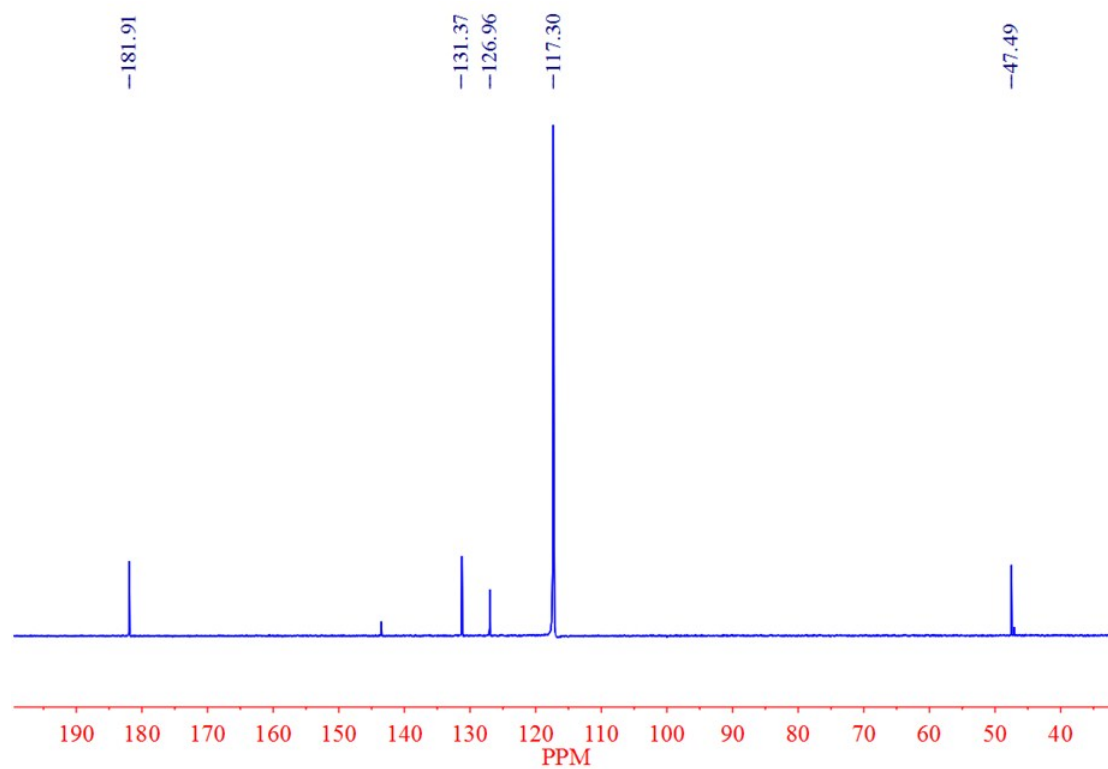


Figure S2. ¹³C NMR spectrum of 1,2-di(imidazole-2-carboxaldehyde)ethane

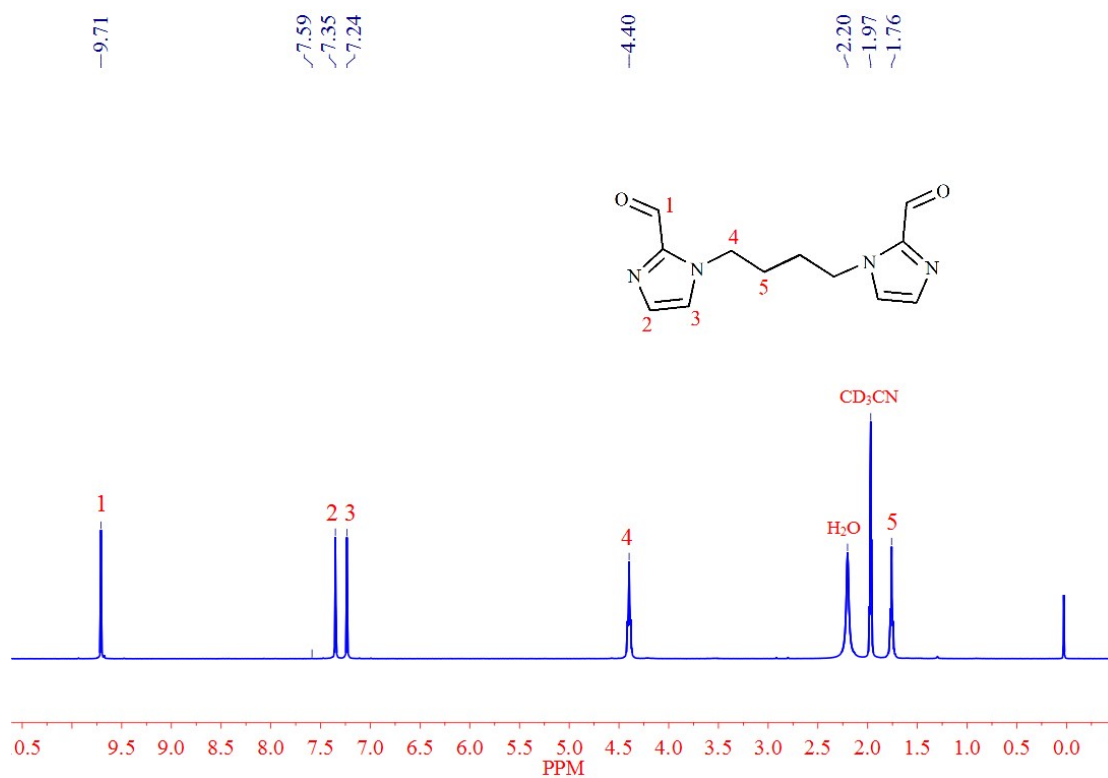


Figure S3. ¹H NMR spectrum of 1,4-di(imidazole-2-carboxaldehyde)butane

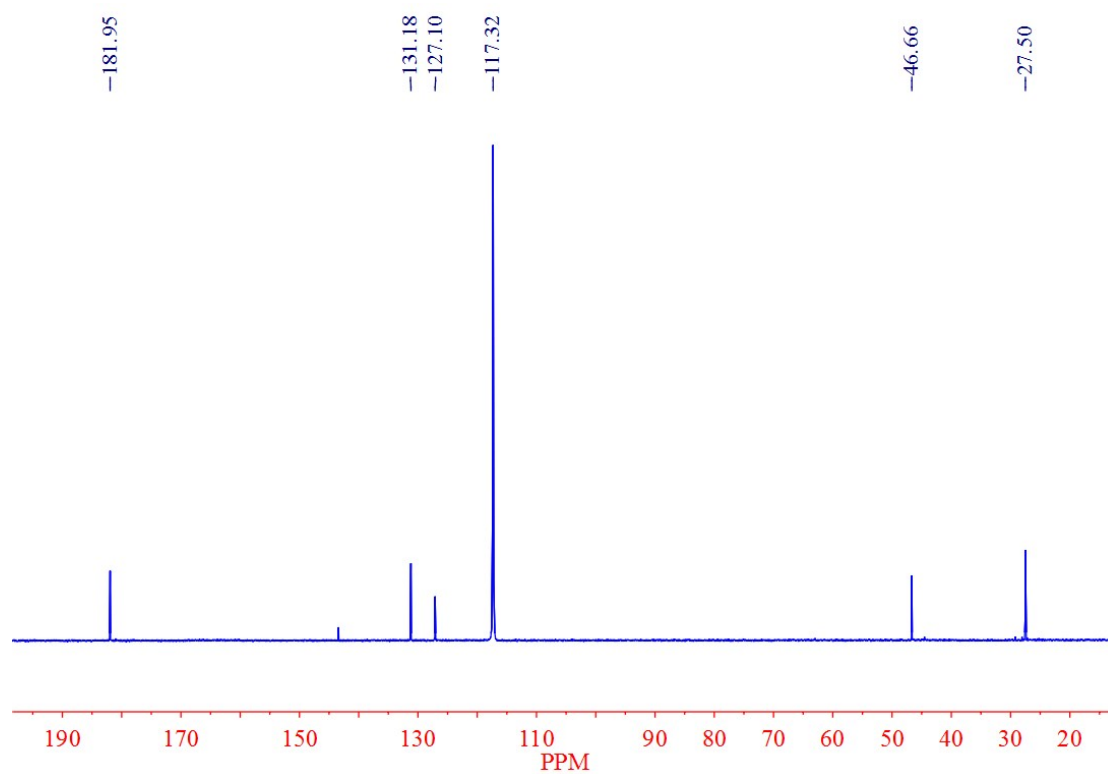


Figure S4. ¹³C NMR spectrum of 1,4-di(imidazole-2-carboxaldehyde)butane

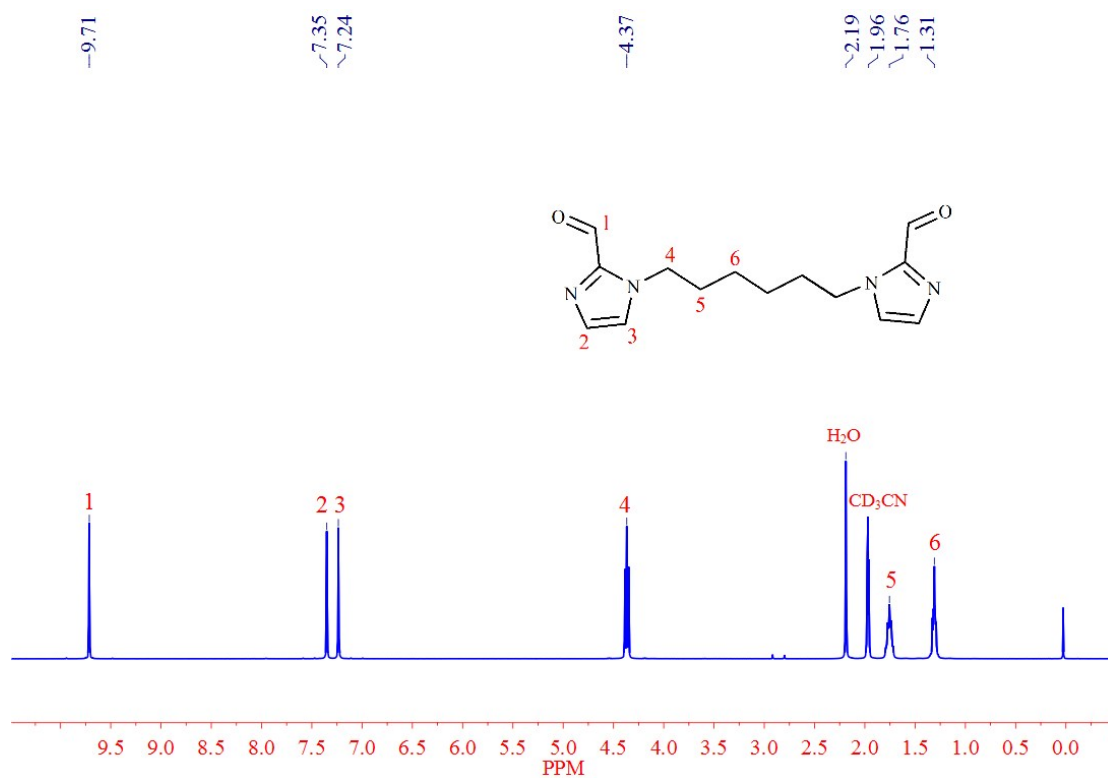


Figure S5. ¹H NMR spectrum of 1,6-di(imidazole-2-carboxaldehyde)hexane

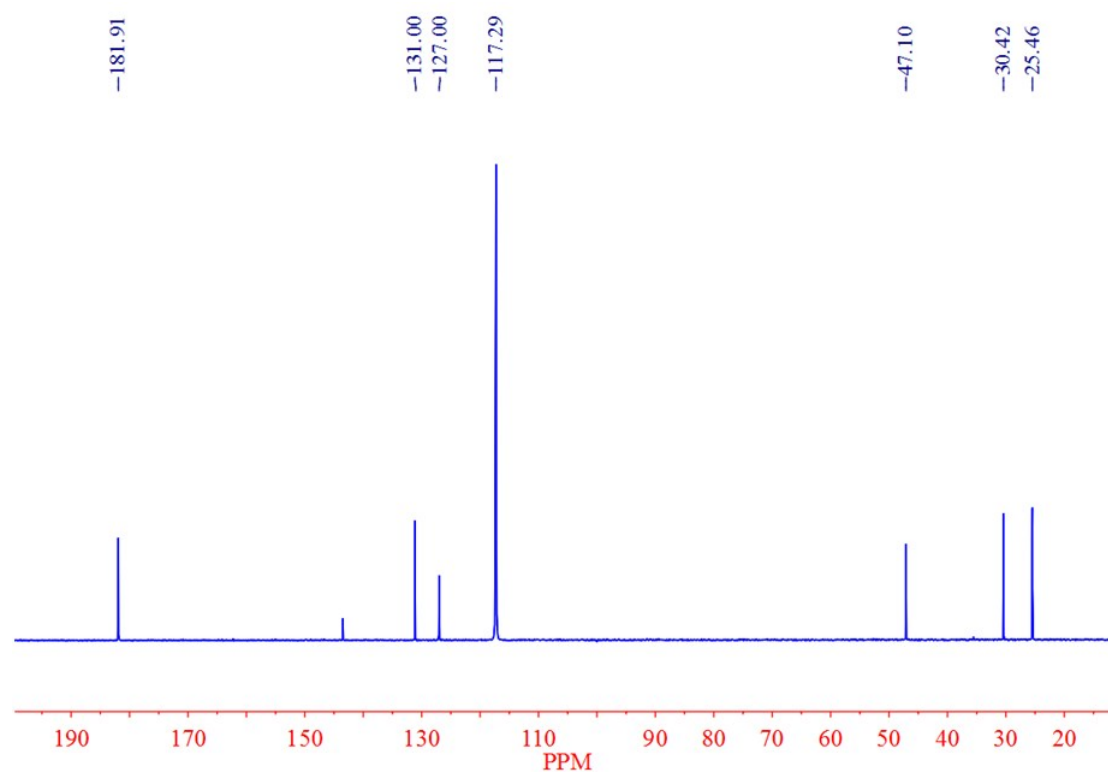


Figure S6. ¹³C NMR spectrum of 1,6-di(imidazole-2-carboxaldehyde)hexane

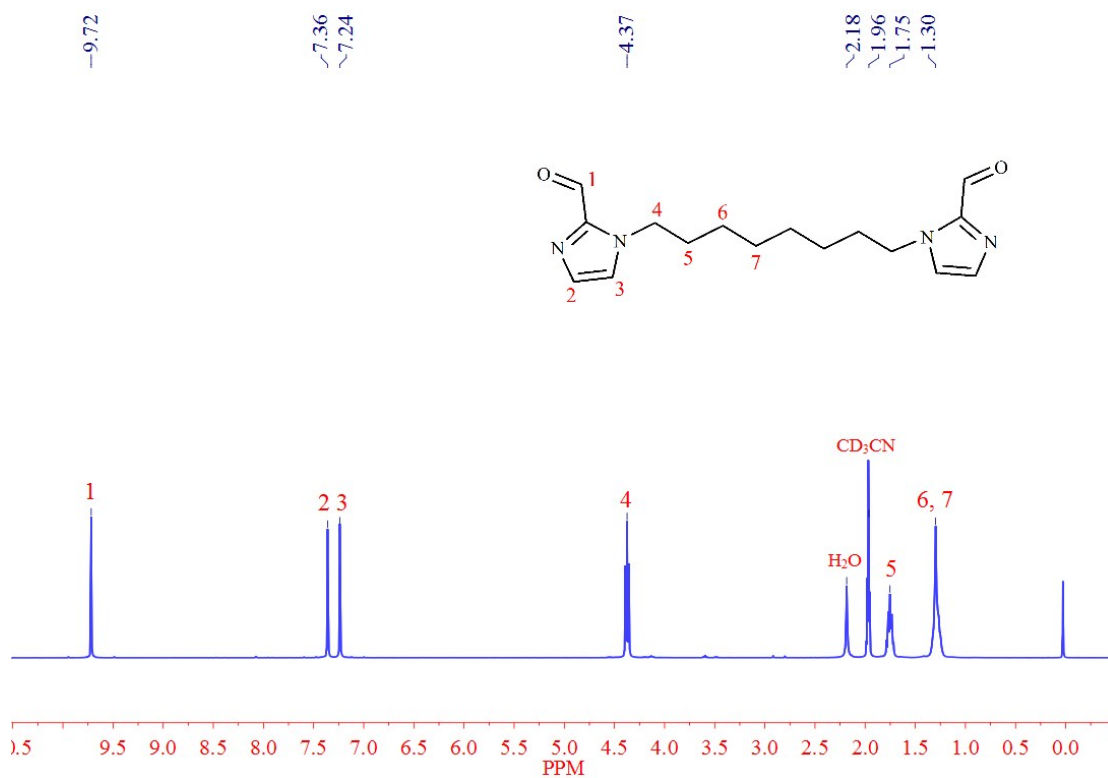


Figure S7. ¹H NMR spectrum of 1,8-di(imidazole-2-carboxaldehyde)octane

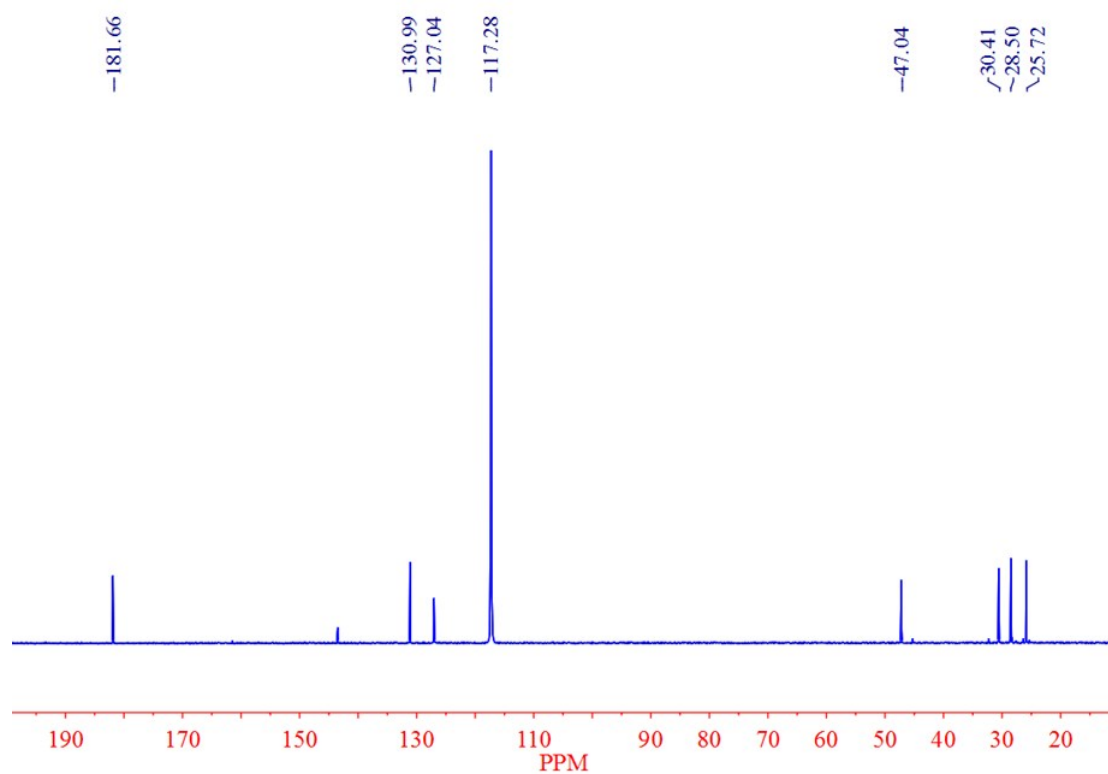


Figure S8. ¹³C NMR spectrum of 1,8-di(imidazole-2-carboxaldehyde)octane

4. Preparation of cages

General procedure for cages *1R* and *1S*

(*R*)-1-(1-naphthyl)ethylamine (68.5 mg, 0.4 mmol) and 1,2-di(imidazole-2-carboxaldehyde)ethane (43.6 mg, 0.2 mmol) were dissolved in 20 mL acetonitrile and heated to reflux for 2 h at 80 °C. After cooling to ambient temperature, solution of NiCl₂·6H₂O (31.6 mg, 0.133 mmol) in 10 mL acetonitrile was added with drops and stirred vigorously for 1 h. The resulting solution was cooled and filtered. Crystalline solid of *1R* was obtained by slow diffusion of diethyl ether into the resulting solution for 1 week. *1S* was prepared following a similar procedure except that (*S*)-1-phenylethylamine instead of (*R*)-1-phenylethylamine was used.

1R: light purple crystals (51%). IR (KBr cm⁻¹): ν = 3055, 2972, 2923, 1604, 1485, 1446, 1384, 1297, 1168, 1103, 1002, 910, 858, 781, 572; Anal. Calcd (%) for Ni₄C₂₀₄N₃₆H₁₉₂Cl₈: C, 66.83; H, 5.28; N, 13.75; Found: C, 66.76; H, 5.31; N, 13.73.

1S: light purple crystals (49%). IR (KBr cm⁻¹): ν = 3053, 2974, 2869, 1618, 1485, 1487, 1446, 1388, 1296, 1166, 1130, 1095, 1002, 968, 914, 860, 783, 578; Anal. Calcd (%) for Ni₄C₂₀₄N₃₆H₁₉₂Cl₈: C, 66.83; H, 5.28; N, 13.75; Found: C, 66.81; H, 5.30; N, 13.77.

General procedure for cages *2R* and *2S*

2R and *2S* were synthesised using the procedure described for *1R* and *1S*, substituting 1,4-di(imidazole-2-carboxaldehyde)butane for 1,2-di(imidazole-2-carboxaldehyde)ethane.

2R: light purple crystals (48%). IR (KBr cm⁻¹): ν = 3051, 2927, 2862, 1610, 1490, 1442, 1380, 1305, 1161, 1101, 999, 966, 914, 860, 779, 576; Anal. Calcd (%) for Ni₄C₂₁₆N₃₆H₂₁₆Cl₈: C, 67.65; H, 5.68; N, 13.15; Found: C, 67.62; H, 5.70; N, 13.17.

2S: light purple crystals (45%). IR (KBr cm⁻¹): ν = 3051, 2968, 2923, 1616, 1494, 1444, 1382, 1307, 1161, 1101, 1002, 970, 916, 858, 781, 574; Anal. Calcd (%) for Ni₄C₂₁₆N₃₆H₂₁₆Cl₈: C, 67.65; H, 5.68; N, 13.15; Found: C, 67.64; H, 5.67; N, 13.16.

General procedure for cages **3R** and **3S**

3R and **3S** were synthesised using the procedure described for **2R** and **2S**, substituting 1,6-di(imidazole-2-carboxaldehyde)hexane for 1,4-di(imidazole-2-carboxaldehyde)butane.

3R: light purple crystals (47%). IR (KBr cm^{-1}): $\nu = 3053, 2925, 2854, 1614, 1488, 1444, 1386, 1309, 1166, 1095, 1000, 970, 912, 860, 781, 572$; Anal. Calcd (%) for $\text{Ni}_4\text{C}_{228}\text{N}_{36}\text{H}_{240}\text{Cl}_8$: C, 68.41; H, 6.04; N, 12.60; Found: C, 68.47; H, 6.02; N, 12.63.

3S: light purple crystals (46%). IR (KBr cm^{-1}): $\nu = 3049, 2929, 2856, 1614, 1490, 1442, 1380, 1309, 1168, 1095, 1000, 966, 914, 856, 779, 574$; Anal. Calcd (%) for $\text{Ni}_4\text{C}_{228}\text{N}_{36}\text{H}_{240}\text{Cl}_8$: C, 68.41; H, 6.04; N, 12.60; Found: C, 68.44; H, 6.05; N, 12.61.

General procedure for cages **4R** and **4S**

4R and **4S** were synthesised using the procedure described for **3R** and **3S**, substituting 1,8-di(imidazole-2-carboxaldehyde)octane for 1,6-di(imidazole-2-carboxaldehyde)hexane.

4R: light purple crystals (52%). IR (KBr cm^{-1}): $\nu = 3053, 2927, 2854, 1614, 1488, 1442, 1375, 1290, 1164, 1101, 1002, 964, 916, 860, 779, 574$; Anal. Calcd (%) for $\text{Ni}_4\text{C}_{240}\text{N}_{36}\text{H}_{264}\text{Cl}_8$: C, 69.11; H, 6.38; N, 12.09; Found: C, 69.12; H, 6.40; N, 12.07.

4S: light purple crystals (50%). IR (KBr cm^{-1}): $\nu = 3051, 2927, 2854, 1616, 1488, 1442, 1377, 1297, 1166, 1103, 1002, 970, 914, 858, 779, 574$; Anal. Calcd (%) for $\text{Ni}_4\text{C}_{240}\text{N}_{36}\text{H}_{264}\text{Cl}_8$: C, 69.11; H, 6.38; N, 12.09; Found: C, 69.14; H, 6.36; N, 12.11.

5. Mass spectra of cages

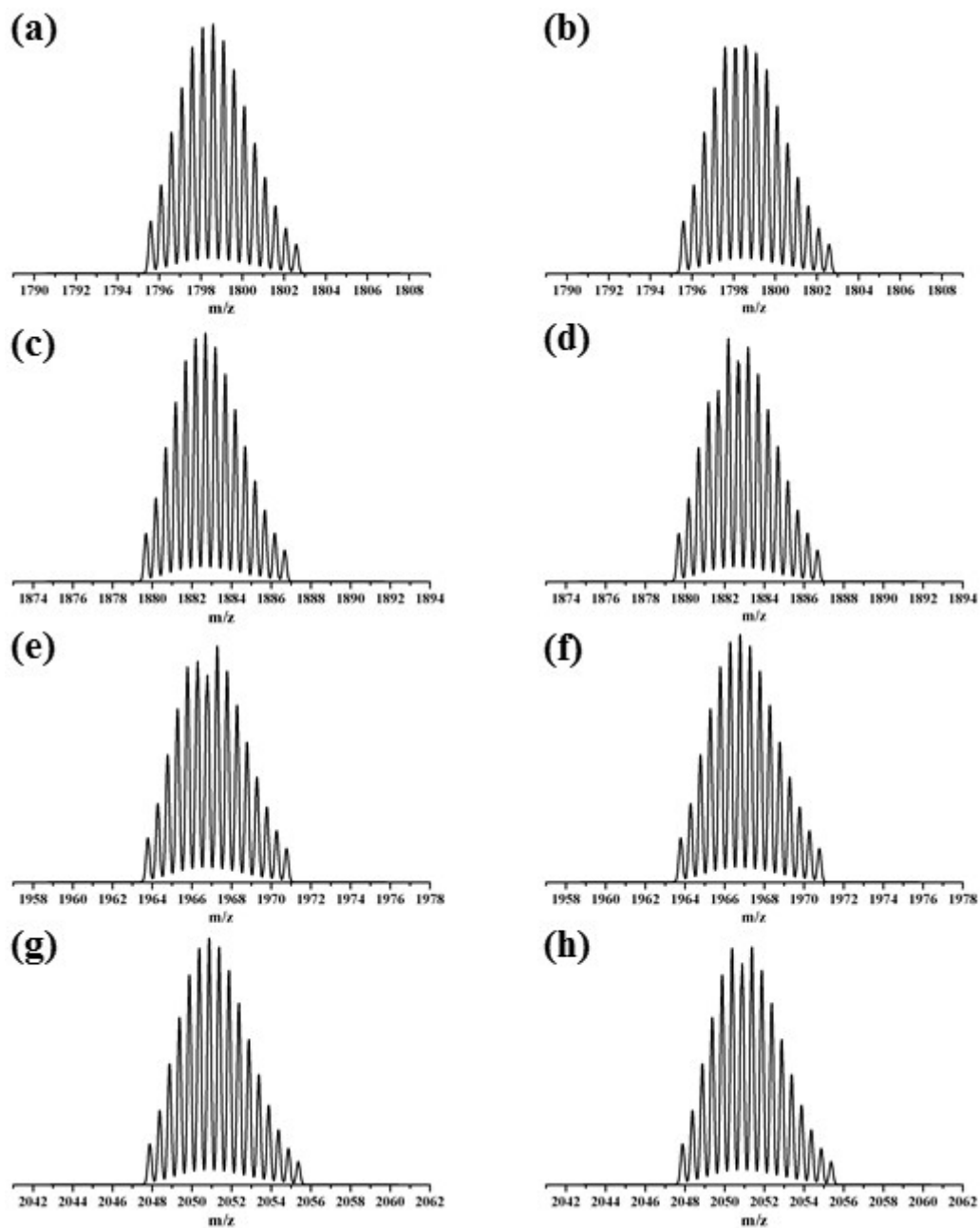


Figure S9. Observed isotope patterns of (a) $[1R(Cl)_6]^{2+}$, (b) $[1S(Cl)_6]^{2+}$, (c) $[2R(Cl)_6]^{2+}$, (d) $[2S(Cl)_6]^{2+}$, (e) $[3R(Cl)_6]^{2+}$, (f) $[3S(Cl)_6]^{2+}$, (g) $[4R(Cl)_6]^{2+}$, (h) $[4S(Cl)_6]^{2+}$.

6. Stability in aqueous media

Visible absorbance spectra for stability studies were recorded using a Shimadzu UV-2101 PC scanning spectrometer. Measurements were collected in a 1 cm path-length cuvette and the standard parameters used were bandwidth 1 nm, response time 1 sec, wavelength scan range 200-400 nm. Visible absorbance spectra for each sample were repeated at least three times. The intensity of the band (200-300 nm) of a 0.01 mM solution of each cage was measured over time in buffer solution at 20 °C (every day for 10 days), since peaks for decomposition products are unlikely to appear in this region. The half-lives ($t_{1/2}$) were calculated using the following equations:

$$\ln[A] = -kt + \ln[A_0]$$

$$t_{1/2} = \frac{\ln(2)}{k}$$

Table S1. Solution half-life ($t_{1/2}$) of the cages (0.01 mM) in buffer solution at 20 °C.

Compound	$t_{1/2}/d$
1R	19.23
1S	23.81
2R	16.21
2S	15.10
3R	17.09
3S	17.58
4R	70.23
4S	50.37

7. CD study of A β peptide interacting with cages

Circular dichroism spectra for property studies were collected using Bio-Logic MOS-450. The spectra of the A β peptide were recorded after interaction with each cage. The A β peptide concentration was 50 μ M and the cages concentrations were 10 μ M. The samples were measured in buffer solution (pH 7.4) after incubation at 37 $^{\circ}$ C for 7 days. Measurements were collected using a 0.2 cm path-length quartz cuvette. The standard parameters used were bandwidth 1 nm, response time 1 sec, wavelength scan range 190-250 nm. For each cage, the solutions were scanned repeatedly, and three scans were automatically averaged. The compound's solvent, DMSO, may have a certain effect on peak shape. However, it was clearly observed that the intensity of the peaks was significantly reduced.

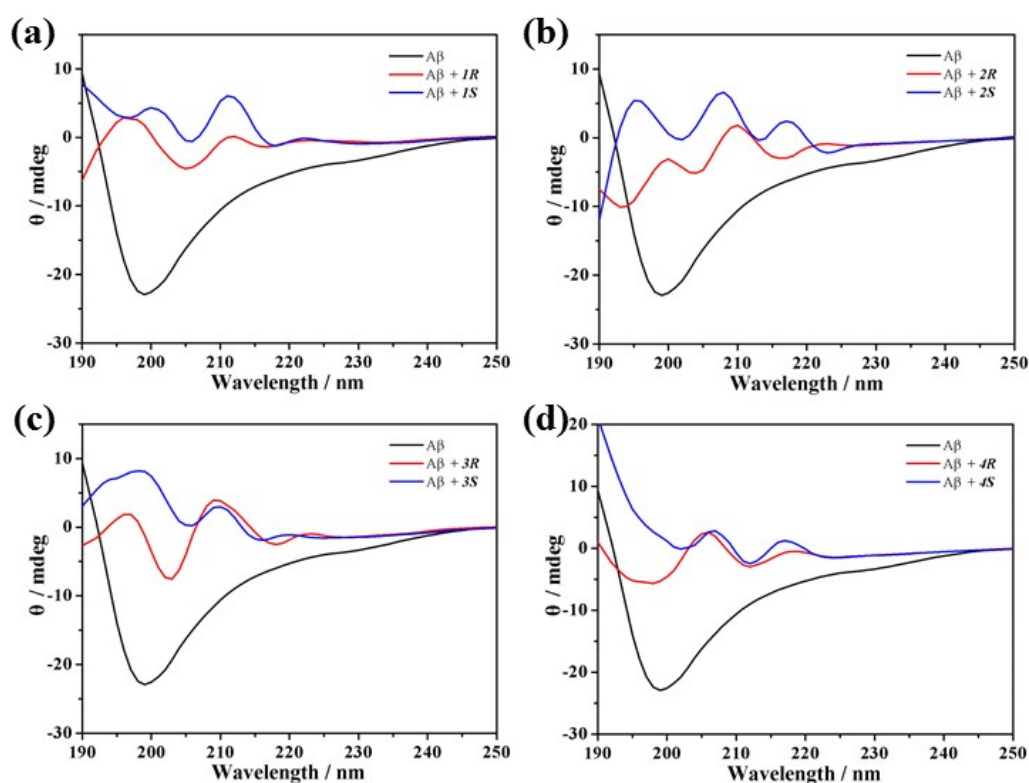


Figure S10. CD spectra of A β peptide in the absence (black) or presence of (a) *1R/1S*, (b) *2R/2S*, (c) *3R/3S*, (d) *4R/4S*. 50 μ M A β peptide or 5:1 mixture of A β peptide and cages were incubated at 37 $^{\circ}$ C for 7 days.

8. AFM images

Atomic Force Microscope (AFM) for morphology studies were collected using Bruker MultiMode 8. The images of the A β peptide were recorded after interaction with each cage. Both A β peptide and the cages concentrations were 50 μ M. They were incubated in buffer solution (pH 7.4) at 37 °C for 7 days and were diluted 50 times with deionized H₂O. Each sample was dropped into fresh mica substrate. After incubation for 5 min, the substrate was rinsed twice with water and allowed to dry. Tapping mode was used to acquire the images. From the AFM images in Figure S11, there are almost no aggregations after the interaction between A β peptide and cages 2, 3 or 4. Some sporadic "dots" have no obvious relationship with the inhibition ability of the cages.

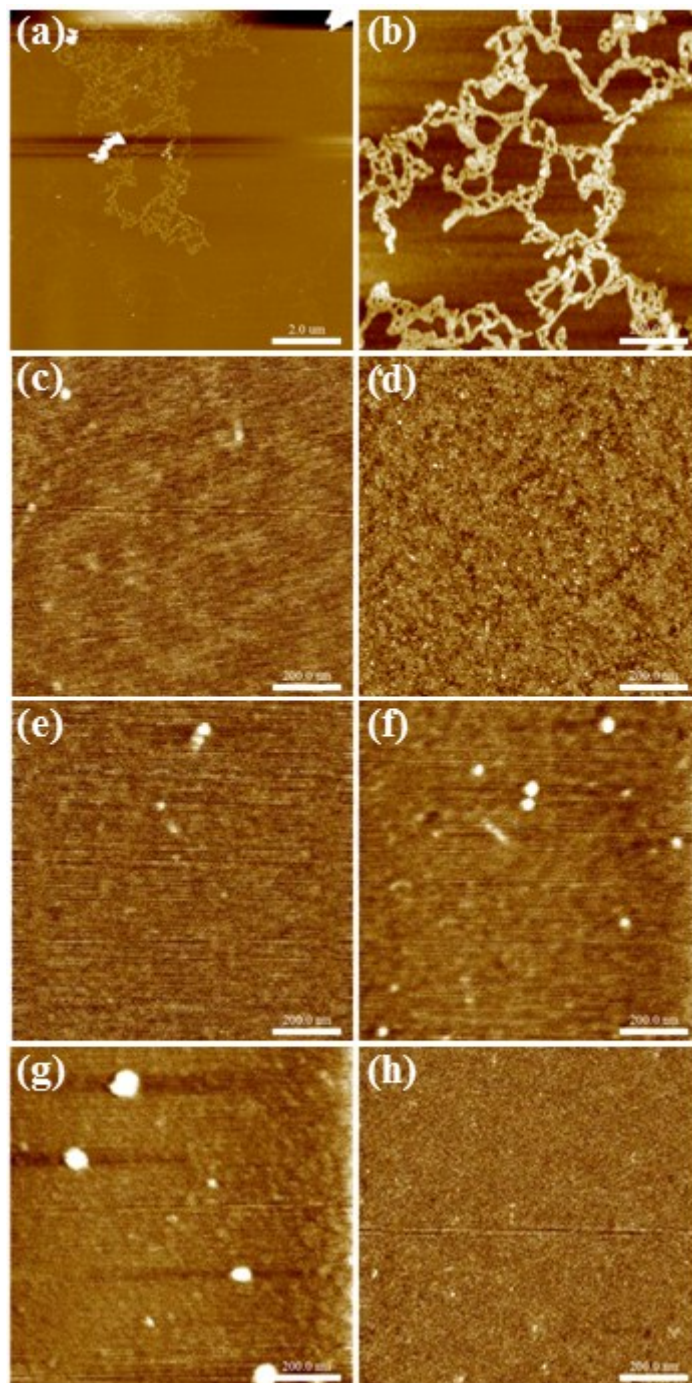


Figure S11. AFM images of A β peptide (a) area corresponding to 10 $\mu\text{m} \times 10 \mu\text{m}$, (b) area corresponding to 1 $\mu\text{m} \times 1 \mu\text{m}$, and the presence of (c) *2R*, (d) *2S*, (e) *3R*, (f) *3S*, (g) *4R*, (h) *4S*. 50 μM A β peptide or 1:1 mixture of A β peptide and cages were incubated at 37 $^{\circ}\text{C}$ for 7 days.

9. Thioflavin T fluorescence assay

Thioflavin T fluorescence assay for aggregation studies were collected using Agilent Cary Eclipse. The fluorescence intensity of the ThT were recorded, which reflected the extent of A β aggregation accurately. The A β peptide concentration was 50 μ M and the cages concentrations were 10 μ M, 20 μ M, 30 μ M, 40 μ M, 50 μ M, 100 μ M, 150 μ M, 200 μ M, respectively. The samples were measured in buffer solution (pH 7.4) after incubation at 37 $^{\circ}$ C for 7 days. Measurements were collected using a 0.5 cm path-length quartz cuvette. The excitation wavelength was 444 nm and the emission at 485 nm was used for analysis. Each data had three parallel tests and the averages were shown in Figure S12.

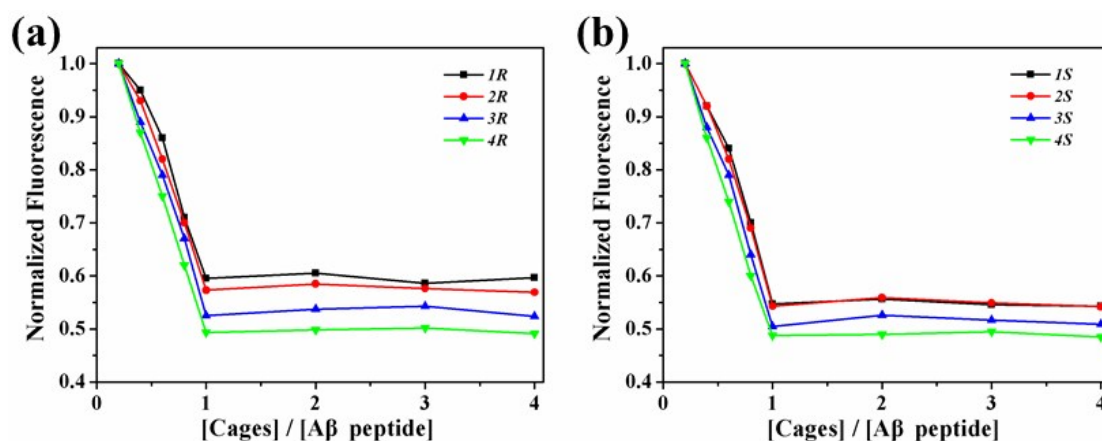


Figure S12. Thioflavin T fluorescence assay measured the cages (a) *1R/2R/3R/4R*, (b) *1S/2S/3S/4S* and A β peptide reaction ratio with different concentration proportions.

10. Effect of the cages on ThT fluorescence

Thioflavin T fluorescence assay was used as described above. The same concentration of ThT was mixed with different cages. After 5 minutes, fluorescence intensity was detected.

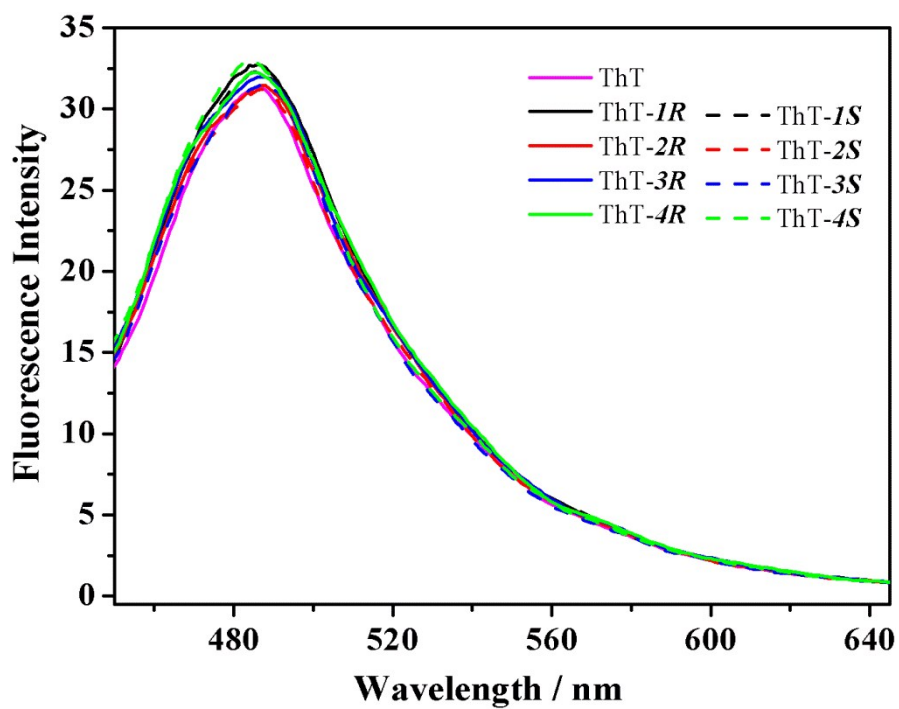


Figure S13. The influence of the cages on the fluorescence of ThT.

11. X-ray crystallography data

The crystal structures were determined on a Siemens (Bruker) SMART CCD diffractometer using monochromated Mo $K\alpha$ radiation ($\lambda = 0.71073 \text{ \AA}$) at 173(2) K. Cell parameters were retrieved using SMART software and refined using SAINT4 on all observed reflections. The highly redundant data sets were reduced using SAINT and corrected for Lorentz and polarization effects. Data was collected using a narrow-frame method with scan widths of 0.30° in ω and an exposure time of 10 s/frame. Absorption corrections were applied using SADABS⁵ supplied by Bruker. Structures were solved by direct methods using the program SHELXL-97⁶. All of the non-hydrogen atoms except the disordered solvent molecules and anions were refined with anisotropic thermal displacement coefficients. Hydrogen atoms of organic ligands were located geometrically and refined in a riding model, whereas those of solvent molecules were not treated during the structural refinements. Disorder was modelled using standard crystallographic methods including constraints, restraints and rigid bodies where necessary. The crystals of the cages **1R**, **2R** and **3S** decayed rapidly out of solvent. Despite rapid handling and long exposure times, the data collected are less than ideal quality. Nevertheless, the data for the cages are of more than sufficient quality to unambiguously establish the connectivity of the structures. Reflecting the instability of the crystals, there is a large area of smeared electron density present in the lattice. Despite many attempts to model this region of disorder as a combination of solvent molecules and partial anions no reasonable fit could be found and accordingly this region was treated with the SQUEEZE function of PLATON. Table S2 lists the crystallographic parameters concerning data collection and structure refinements for the cages, while selected bond distances and angles are given in Table S3.

Table S2. Summary of crystallographic data for cages.

	<i>1R</i>	<i>2R</i>	<i>3S</i>
formula	C ₂₀₄ H ₁₉₂ B ₅ F ₂₀ N ₃₆ Ni ₄	C ₂₁₆ H ₂₁₆ Cl ₅ N ₃₆ Ni ₄ O ₂₀	C ₂₂₈ H ₂₄₀ N ₃₆ Ni ₄
fw	3816.83	4048.34	3719.39
<i>T</i> (K)	123(2)	173(2)	173(2)
λ (Å)	0.71073	0.71073	0.71073
crystal system	Orthorhombic	Cubic	Cubic
space group	<i>I</i> 222	<i>I</i> 23	<i>I</i> 23
<i>a</i> (Å)	19.7257(11)	22.4671(11)	23.8389(14)
<i>b</i> (Å)	25.1015(19)	22.4671(11)	23.8389(14)
<i>c</i> (Å)	25.7068(17)	22.4671(11)	23.8389(14)
α (°)	90	90	90
β (°)	90	90	90
γ (°)	90	90	90
<i>V</i> (Å ³)	12728.6(15)	11340.7(10)	13548(2)
<i>Z</i>	2	2	2
<i>D</i> _{calc} (Mg/m ³)	0.996	1.186	0.912
μ (mm ⁻¹)	0.354	0.452	0.321
<i>F</i> (000)	3970	4242	3944
θ (°)	1.13- 23.81	3.14-23.23	3.0-23.2
index ranges	□21<= <i>h</i> <=21	□23<= <i>h</i> <=10	□22<= <i>h</i> <=26
	□28<= <i>k</i> <=21	□23<= <i>k</i> <=23	□7<= <i>k</i> <=23
	□29<= <i>l</i> <=28	□24<= <i>l</i> <=21	□25<= <i>l</i> <=26
reflections collected	20080	6250	8663
GOF (<i>F</i> ²)	1.102	1.108	1.038
<i>R</i> _{<i>f</i>} ^{<i>a</i>} , <i>wR</i> ₂ ^{<i>b</i>} (<i>I</i> >2 σ (<i>I</i>))	0.0964, 0.2217	0.0811, 0.1976	0.0799, 0.2035
<i>R</i> _{<i>f</i>} ^{<i>a</i>} , <i>wR</i> ₂ ^{<i>b</i>} (all data)	0.1624, 0.2445	0.1439, 0.2230	0.1814, 0.2549

$$R_f^a = \frac{\sum ||F_o| - |F_c||}{\sum F_o}, \quad wR_2^b = [\frac{\sum w(F_o^2 - F_c^2)^2}{\sum w(F_o^2)}]^{1/2}$$

Table S3. Selected bond lengths [Å] and angles [°] for cages.

<i>1R</i>			
N(1C)-Ni(1)#1	2.244(18)	N(3C)-Ni(1)#1	2.347(15)
N(1X)-Ni(1)	1.882(17)	N(3X)-Ni(1)	1.998(12)
N(1A)-Ni(1)	1.940(7)	N(3A)-Ni(1)	2.187(8)
N(1B)-Ni(1)	2.009(8)	N(3B)-Ni(1)	2.139(9)
Ni(1)-N(1C)#1	2.244(18)	Ni(1)-N(3C)#1	2.347(15)
N(1X)-Ni(1)-N(1A)	90.2(4)	N(1X)-Ni(1)-N(3X)	84.2(6)
N(1A)-Ni(1)-N(3X)	173.0(5)	N(1X)-Ni(1)-N(1B)	93.3(6)
N(1A)-Ni(1)-N(1B)	88.7(3)	N(3X)-Ni(1)-N(1B)	95.8(5)
N(1X)-Ni(1)-N(3B)	170.2(6)	N(1A)-Ni(1)-N(3B)	95.0(3)
N(3X)-Ni(1)-N(3B)	91.1(5)	N(1B)-Ni(1)-N(3B)	78.6(4)
N(1X)-Ni(1)-N(3A)	91.4(6)	N(1A)-Ni(1)-N(3A)	78.5(3)
N(3X)-Ni(1)-N(3A)	97.4(5)	N(1B)-Ni(1)-N(3A)	166.4(3)
N(3B)-Ni(1)-N(3A)	97.8(3)	N(1X)-Ni(1)-N(1C)#1	4.1(9)
N(1A)-Ni(1)-N(1C)#1	91.4(4)	N(3X)-Ni(1)-N(1C)#1	83.3(6)
N(1B)-Ni(1)-N(1C)#1	89.4(6)	N(3B)-Ni(1)-N(1C)#1	166.2(5)
N(3A)-Ni(1)-N(1C)#1	95.4(5)	N(1X)-Ni(1)-N(3C)#1	70.9(5)
N(1A)-Ni(1)-N(3C)#1	160.9(5)	N(3X)-Ni(1)-N(3C)#1	13.5(4)
N(1B)-Ni(1)-N(3C)#1	94.6(4)	N(3B)-Ni(1)-N(3C)#1	104.1(4)
N(3A)-Ni(1)-N(3C)#1	99.0(4)	N(1C)#1-Ni(1)-N(3C)#1	69.9(5)
<i>2R</i>			
N(1)-Ni(1)	2.036(8)	N(3)-Ni(1)	2.152(7)
Ni(1)-N(1)#13	2.036(8)	Ni(1)-N(1)#14	2.036(8)
Ni(1)-N(3)#14	2.152(7)	Ni(1)-N(3)#13	2.152(7)
N(1)-Ni(1)-N(1)#13	91.8(4)	N(1)-Ni(1)-N(1)#14	91.8(4)
N(1)#13-Ni(1)-N(1)#14	91.8(4)	N(1)-Ni(1)-N(3)#14	95.7(3)
N(1)#13-Ni(1)-N(3)#14	168.9(3)	N(1)#14-Ni(1)-N(3)#14	79.8(3)
N(1)-Ni(1)-N(3)#13	168.9(3)	N(1)#13-Ni(1)-N(3)#13	79.8(3)
N(1)#14-Ni(1)-N(3)#13	95.7(3)	N(3)#14-Ni(1)-N(3)#13	93.7(3)
N(1)-Ni(1)-N(3)	79.8(3)	N(1)#13-Ni(1)-N(3)	95.7(3)
N(1)#14-Ni(1)-N(3)	168.9(3)	N(3)#14-Ni(1)-N(3)	93.7(3)
N(3)#13-Ni(1)-N(3)	93.7(3)		
<i>3S</i>			
Ni1-N1	2.00(3)	Ni1-N3	2.14(3)
Ni1-N1'_b	2.21(4)	Ni1-N3'_b	2.20(4)
Ni1-N1'_e	2.00(3)	Ni1-N3'_e	2.14(3)
Ni1-N1'_f	2.21(4)	Ni1-N3'_f	2.20(4)
Ni1-N1'_i	2.21(4)	Ni1-N3'_i	2.20(4)

Ni1-N1_j	2.00(3)	Ni1-N3_j	2.14(3)
N1-Ni1-N3	80.9(11)	N1_j-Ni1-N1'_b	97.8(15)
N1-Ni1-N1'_b	8.4(14)	N1'_b-Ni1-N3_j	96.5(17)
N1-Ni1-N3'_b	83.4(11)	N1_e-Ni1-N3'_b	87.8(16)
N1-Ni1-N1_e	90.2(14)	N3_e-Ni1-N3'_b	94.3(14)
N1-Ni1-N3_e	170.9(14)	N1'_f-Ni1-N3'_b	92.3(17)
N1-Ni1-N1'_f	97.8(15)	N3'_b-Ni1-N3'_f	98.4(14)
N1-Ni1-N3'_f	173.3(13)	N1'_i-Ni1-N3'_b	168.5(14)
N1-Ni1-N1'_i	86.6(15)	N3'_b-Ni1-N3'_i	98.4(14)
N1-Ni1-N3'_i	87.8(16)	N1_j-Ni1-N3'_b	173.3(14)
N1-Ni1-N1_j	90.2(14)	N3_j-Ni1-N3'_b	101.3(15)
N1-Ni1-N3_j	91.7(16)	N1_e-Ni1-N3_e	80.9(11)
N1'_b-Ni1-N3	73.4(13)	N1_e-Ni1-N1'_f	8.4(14)
N3-Ni1-N3'_b	4.6(15)	N1_e-Ni1-N3'_f	83.4(11)
N1_e-Ni1-N3	91.7(16)	N1_e-Ni1-N1'_i	97.8(15)
N3-Ni1-N3_e	97.4(14)	N1_e-Ni1-N3'_i	173.3(14)
N1'_f-Ni1-N3	96.5(17)	N1_e-Ni1-N1_j	90.2(14)
N3-Ni1-N3'_f	101.3(15)	N1_e-Ni1-N3_j	170.9(13)
N1'_i-Ni1-N3	164.3(15)	N1'_f-Ni1-N3_e	73.4(13)
N3-Ni1-N3'_i	94.3(14)	N3_e-Ni1-N3'_f	4.6(15)
N1_j-Ni1-N3	170.9(13)	N1'_i-Ni1-N3_e	96.5(17)
N3-Ni1-N3_j	97.4(14)	N3_e-Ni1-N3'_i	101.3(15)
N1'_b-Ni1-N3'_b	75.7(12)	N1_j-Ni1-N3_e	91.7(16)
N1_e-Ni1-N1'_b	86.6(15)	N3_e-Ni1-N3_j	97.4(14)
N1'_b-Ni1-N3_e	164.3(15)	N1'_f-Ni1-N3'_f	75.7(12)
N1'_b-Ni1-N1'_f	94.6(16)	N1'_f-Ni1-N1'_i	94.6(16)
N1'_b-Ni1-N3'_f	168.5(15)	N1'_f-Ni1-N3'_i	168.5(14)
N1'_b-Ni1-N1'_i	94.6(16)	N1_j-Ni1-N1'_f	86.6(15)
N1'_b-Ni1-N3'_i	92.3(17)	N1'_f-Ni1-N3_j	164.3(15)
N1'_i-Ni1-N3'_f	92.3(17)	N3'_f-Ni1-N3'_i	98.4(14)
N1_j-Ni1-N3'_f	87.8(17)	N3_j-Ni1-N3'_f	94.3(14)
N1'_j-Ni1-N3'_i	75.7(12)	N1_j-Ni1-N1'_i	8.4(14)
N1'_i-Ni1-N3_j	73.4(13)	N1_j-Ni1-N3'_i	83.4(11)
N3_j-Ni1-N3'_i	4.6(15)	N1_j-Ni1-N3_j	80.9(11)

For **1R**: #1 -x+1, -y+2, z;

For **2R**: #13 y, z, x; #14 z, x, y;

For **3S**: b = x, 2-y, 2-z; e = 1-z, 1-x, y; f = -1+z, 1-x, 2-y; i = -1+y, 2-z, 1-x; j = 1-y, z, 1-x;